

Predictability of Large Avalanches on a Sandpile

J. Rosendahl, M. Vekić, and J. E. Rutledge

Department of Physics, University of California, Irvine, California 92717

(Received 11 March 1994)

When grains are added to a large sandpile, quasiperiodic large avalanches maintain the steady state mass. The buildup periods between the large avalanches contain many small avalanches. The size distribution of the small events does not vary during a buildup period but their mean rate of occurrence does. The qualitative behavior of the real sandpile avalanches is identical to the behavior of earthquakes on a model fault proposed by Carlson and Langer. As that model suggests, the running total number of small avalanches can in principle predict the occurrence of the large avalanches.

PACS numbers: 46.10.+z, 05.40.+j, 91.30.Px

Earthquake faults and sandpiles are examples of extended dynamical systems. Computer model earthquake faults replicate many features of the seismic activity on at least some real earthquake faults [1,2]. A model fault consists of massive blocks coupled to one another and to a fixed lattice by springs. The blocks are in contact with a plate and are driven by friction as the plate slides past them. A model earthquake results when blocks break free and slide along the plate. One of the uses of these models is to study the predictability of large, catastrophic earthquakes [3,4]. Some of this work suggests that the sequence of small earthquakes might be used to predict the time and place of major events [3].

We have measured the time dependence of the total mass of a real conical sandpile as individual grains are added to it. The addition of sand grains to the pile causes occasional avalanches that carry grains off the pile. The avalanches vary in size from a few grains to slides that remove roughly one-third of the surface layer from the pile. Avalanches on a sandpile are the analogs of earthquakes on a real fault or block slides in the model fault. We have found that features of avalanches on large piles are qualitatively identical to their analogs in the model earthquake fault as discussed by Shaw, Carlson, and Langer [3]. Furthermore, like small events on the model fault, the time evolution of small avalanches on a real sandpile can in principle be used to predict the arrival of large avalanches.

Our experimental technique [5] is similar to the one reported by Held *et al.* [6]. The mass of a conical sandpile is monitored as grains are added to it. When the mass changes by at least the mass of one grain, an event is said to take place. The mass of the pile is recorded and the time advances by one unit. We measure time in events so the effective stress grows linearly when unrelieved by avalanches. Our technique is insensitive to sand slides that are entirely contained on the pile.

The avalanches on our sandpile are typical of the avalanches seen previously on large piles. Large piles have linear dimensions of at least 50 times the grain diameter [7]. Typically large piles show quasiperiodic major

avalanches [5,6,8,9] separated by periods containing numerous small avalanches [5,9]. Figure 1 shows the number of grains on the pile through almost 52 500 events. An arbitrary number of grains ($\sim 80\,000$) has been subtracted so that the fluctuations in the mass can be clearly seen. Twelve abrupt decreases of between 2000 and 6000 grains occurring in a single time step are the most striking feature. These are the major avalanches. Preceding each major avalanche is a buildup period during which the addition of a single grain to the pile is the most common event. However, on the average each buildup period contains 110 small avalanches. They are more effective in removing mass from the pile at the end of the buildup period as can be seen by the decrease of the mean slope of each buildup period as a major avalanche is approached. In the data set there are 11 complete cycles consisting of a buildup period and a major avalanche.

The size distribution of all 1189 avalanches in the 11 complete cycles is shown in Fig. 2(a). Because of their sparsity, the data are binned for avalanches of 13 grains and larger. The number plotted is the logarithm of the number of avalanches in each bin divided by the total number of avalanches and by the width of the bin. It is the probability per unit size averaged across the bin width.

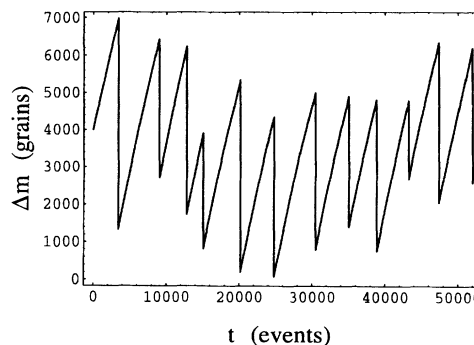


FIG. 1. The mass of the sandpile as a function of time in events. An event is a detected mass change. Large avalanches are separated by buildup periods. Events that remove mass become more frequent as a buildup period progresses.

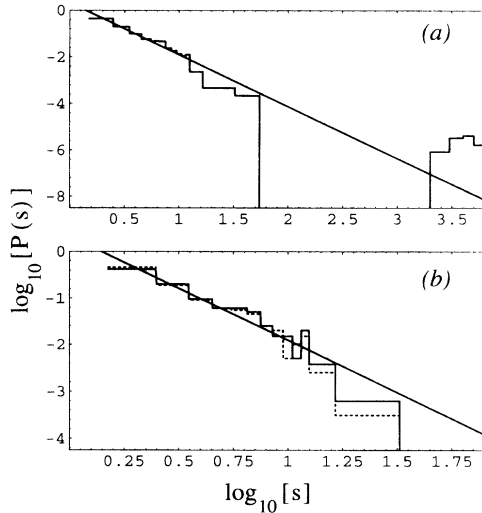


FIG. 2. Size distributions of avalanches of size s grains. (a) All avalanches. For small avalanches the distribution is a power law, shown by the line. There is an excess of large avalanches. (b) The dotted lines show the distribution of the first $\frac{1}{6}$ of the avalanches in each buildup period; the solid lines show the distribution of the last $\frac{1}{6}$ of the avalanches in each buildup period. The straight line is the same line in (a). Within statistical scatter, these distributions are the same and the same as the distribution of small avalanches in (a).

Also shown is a power law distribution with a slope of -2.23 . Avalanches between 2 and 55 grains are distributed according to this power law. The small avalanches on large, uniformly rotated sandpiles follow a power law with nearly the same exponent [9]. No avalanches in the range from 56 to 2111 grains occurred. Had the avalanches in this range been distributed according to the same power law as the small ones, there would have been 12 of them. There are 11 avalanches in the bins between 2000 and 6000 grains, 2 orders of magnitude more than expected from the extrapolated power law. Overly frequent large events are seen in models of earthquake faults [1] and sandpiles [10] that take inertia into account, and in the size distribution of real earthquakes [11].

The small avalanches remove more mass per unit time during the later part of a period because they become more frequent, not because they become larger. The dotted curve in Fig. 2(b) shows the size distribution of the first $\frac{1}{6}$ of the avalanches in each cycle. The solid curve is the size distribution of the last $\frac{1}{6}$ of the avalanches in each cycle. The straight line is the -2.23 power law of Fig. 2(a). Neither inspection of the two distributions nor comparison of either with the distribution of all avalanches in Fig. 2(a) forces the conclusion that the size distribution changes as a buildup period progresses. This impression is confirmed by the relevant statistical test [12].

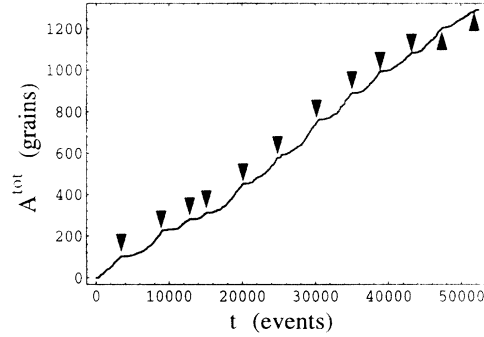


FIG. 3. A^{tot} vs t for the data shown in Fig. 1. A^{tot} is the running total number of avalanches. The curves become steeper during each buildup period showing that the rate of small avalanches increases as a major avalanche is approached.

Figure 3 shows the running total number of avalanches versus time for all the data in Fig. 1. We will call this quantity the total activity A^{tot} . The times of the major avalanches are shown by the black triangles. During all 11 buildup periods the coarse-grained average slope of the total activity versus time, the coarse-grained avalanche rate, smoothly increases. This accounts for the increased flow rate off the pile as the end of a cycle is approached.

To examine the time sequences of small avalanches more closely we will examine the running total number of avalanches in each cycle. We calculate the running total number of avalanches versus time beginning both from zero just after a major avalanche and ending just before the next large event. It is convenient to convert these data into a continuous function of time by extrapolating straight lines through successive discrete data points. Normalizing the resulting function by dividing the time by the length of the period and the running total number of avalanches by the total number at the end of the cycle creates normalized total activities $a_n(\tau)$. Here n is the cycle number and τ the normalized time. Both run from 0 to 1 for each n . The average of all 11 a_n is shown in Fig. 4 along with a smooth curve, a graph of τ^2 . The average rate of small avalanches, the derivative of the curve in Fig. 4, increases linearly from zero between major events. The time evolution of avalanches on conical piles and on uniformly rotated sand slopes are different [9]. It is not clear whether the difference is due to the different geometries of the piles or the different driving mechanisms in the two experiments.

The qualitative behavior of the avalanche data shown in Figs. 2, 3, and 4 is strikingly similar to the behavior of earthquakes on the model fault of Carlson and Langer [13]. Like the avalanches, the model earthquakes show a power law distribution of small quakes and an excess of major earthquakes. The size distribution of model earthquakes varies only weakly across a cycle, and the rate of small earthquakes increases between major

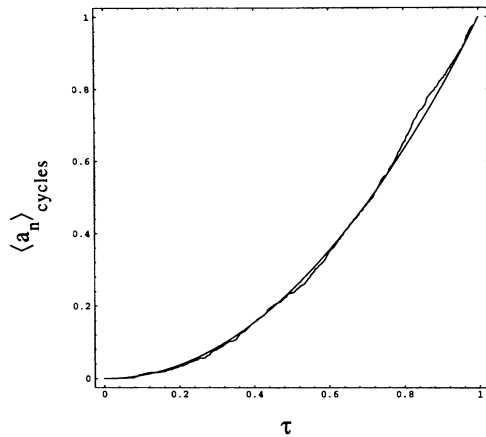


FIG. 4. The normalized total activity during a single cycle averaged over all 11 complete buildup periods. The smooth curve is τ^2 . The average avalanche rate grows linearly during each buildup period.

quakes. Sandpile and fault models differ quantitatively. The model earthquakes have an inverse size distribution, consistent with the Gutenberg-Richter law [14]. The curvature of the average normalized total activity is much stronger for the model earthquakes than it is for the real avalanches. Nevertheless, the qualitative similarity of the two systems suggests that inferences drawn from the earthquake model might apply to sandpile data.

Major avalanche prediction is an example. The lengths of the buildup periods and the total activity at the end of each cycle are broadly dispersed. The cycle lengths vary from 2268 events to 5627 events, and the total activity at the end of a cycle varies from 29 to 183 avalanches. By themselves these numbers are weak indicators of the completeness of a cycle. However, the running total number of small avalanches seems correlated with the arrival of major avalanches, as seen in Fig. 4. Based on similar behavior of the total earthquake activity generated by the model, Shaw, Carlson, and Langer [3] have remarked that these functions are useful predictors of major earthquakes. We can apply this suggestion to the avalanches on our sandpile.

The total activity can be used to predict major avalanches only if the total activity beginning at the start of a buildup period and ending at an arbitrary time during a cycle is distinguishable from a complete cycle total activity. A reasonably reliable assessment of the completeness of the total activity can be made. If the a_n are plotted on the same axes, they divide the τ - a_n plane into two regions. One region lies between the upper and lower envelopes of all the a_n and the other lies outside both envelopes. For clarity a_{11} , a_7 , and a_3 along with τ^2 are shown in Fig. 5(a). Over most of their length a_{11} and a_3 form the upper and lower envelopes for all the a_n . To decide whether a major avalanche is due at an arbitrary

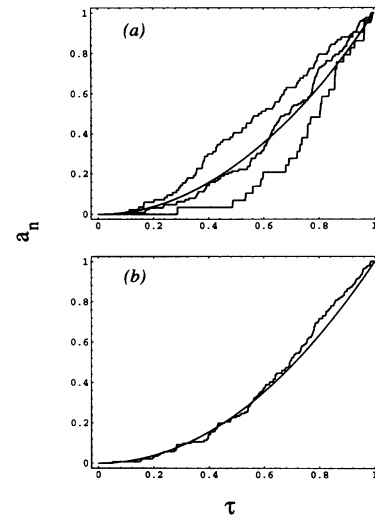


FIG. 5. (a) Normalized total activities for cycles 11, 7, and 3 (top to bottom). If normalized total activities were plotted for all 11 cycles, the curves would lie between the upper and lower curves shown here over nearly the entire time interval. Incomplete segments of these three cycles are rarely classified as complete. (b) Normalized total activity for cycle 4. Incomplete segments of this cycle when normalized are mistaken for complete cycles almost 11% of the time.

time in a buildup cycle, we construct the normalized total activity function from the beginning of the cycle to that time using exactly the procedure that generates the a_n for complete cycles. If that function is entirely contained within the region between the envelopes, it is indistinguishable by our criterion from a complete cycle normalized total activity. We predict that a major event is imminent. Otherwise the cycle is declared incomplete and a major event is not immediately expected. By construction this procedure recognizes actual complete cycles and correctly anticipates all the major avalanches.

The suitability of the total activity as a predictor of large events becomes apparent when the number of incorrectly identified incomplete cycles is examined. For each cycle we have constructed normalized, total activity curves ending between 20% and 100%, in 0.1% steps, of the way through the cycle. Shorter partial cycles contain so few events they are obviously incomplete. Only 2% of the resulting incomplete normalized total activity curves lie between the upper and lower envelopes and are consequently misidentified. In other words, only during scattered short periods totaling 2% of a typical cycle is a major avalanche erroneously anticipated. Cycle 7 in Fig. 5(a) is typical with only 2.1% misidentifications. Like most cycles, the misidentified incomplete activities, or false alarms, occur primarily during the last 20% of the cycle. A small rate of false alarms is not built into the algorithm. Rather it demonstrates the existence of recognizable differences between the partial and complete

cycle total activities. This is significant because if no such differences could be identified, time prediction of major avalanches based on the total activity would be impossible despite the correlation evident in Fig. 3.

If the complete activities followed an exact power law, as the average tends to in Fig. 4, incomplete normalized activities would look identically complete by our criterion. The normalization procedure maps a given power law on the range $[0, t]$ into the same function on the range $[0, 1]$ for all t . The fluctuations from the mean behavior do not map into themselves. Paradoxically the fluctuations are responsible for the spread in the complete cycle normalized activities and the success of the discrimination procedure. Cycle 7 in Fig. 5(a) deviates more from the smooth quadratic curve than does cycle 4 in Fig. 5(b). Cycle 4 contains false alarm periods totaling almost 11% period of the cycle. Even then, they all occur during the last quarter of the cycle.

We have demonstrated that normalized activities from partial avalanche cycles are highly distinguishable from normalized activities from complete cycles. It is likely that more sophisticated recognition techniques can reduce the false alarm rate further. Finally, if modeling of sandpile avalanches could be used to locate the upper and lower envelopes, true major avalanche prediction could be investigated. Establishing a similar scenario is among the goals of fault models [4].

It is remarkable that temporal patterns identified in a fault model are found in a sandpile because the underlying dynamics are very different. The blocks in the fault are bound, interact with each other harmonically, and are driven by a nonlinear external force. The sand grains are unbound, experience only hard core mutual repulsions, and are driven by gravity. Nevertheless, when driven

both systems maintain a steady state by relaxing in similar ways.

-
- [1] J. M. Carlson and J. S. Langer, Phys. Rev. Lett. **62**, 2632 (1989); J. M. Carlson and J. S. Langer, Phys. Rev. A **40**, 6470 (1989).
 - [2] K. Chen, P. Bak, and S. Obukov, Phys. Rev. A **43**, 625 (1991).
 - [3] Bruce E. Shaw, J. M. Carlson, and J. S. Langer, J. Geophys. Res. **97**, 479 (1992).
 - [4] S. L. Pepke, J. M. Carlson, and B. E. Shaw (to be published).
 - [5] J. Rosendahl, M. Vekić, and J. Kelley, Phys. Rev. E **47**, 1401 (1993).
 - [6] G. A. Held, D. H. Solina II, D. T. Keane, W. J. Haag, P. M. Horn, and G. Grinstein, Phys. Rev. Lett. **65**, 381 (1990).
 - [7] Sidney R. Nagel, Rev. Mod. Phys. **64**, 321 (1992).
 - [8] H. M. Jaeger, C.-h. Liu, and S. R. Nagel, Phys. Rev. Lett. **62**, 40 (1989).
 - [9] Michael Bretz, Jevne B. Cunningham, Peter L. Kurczynski, and Franco Nori, Phys. Rev. Lett. **69**, 2431 (1992).
 - [10] Carmen P. C. Prado and Zeev Olami, Phys. Rev. A **45**, 665 (1992).
 - [11] B. E. Shaw, Geophys. Rev. Lett. **20**, 643 (1993).
 - [12] W. H. Press, B. P. Flannery, S. A. Teukolsky, and W. T. Vetterling, *Numerical Recipes* (Cambridge University Press, Cambridge, 1989), pp. 470–472.
 - [13] See Ref. [3]. There is also spatial information in the model that our experiment does not probe.
 - [14] B. Gutenberg and C. F. Richter, *Seismicity of the Earth and Related Phenomena* (Princeton University Press, Princeton, NJ, 1954).